Energy Engineering

Tech Science Press

https://doi.org/10.32604/ee.2026.078724

ARTICLE

Low-Carbon and Economic Dispatch Strategy Considering Optimal Multi-Machine Allocation and Power Control for Grid-Forming Energy Storage in Micro-Energy Grids

Yiqun Kang[1,*], Zhe Li[1], Li You[1], Haozhe Xiong[2], Yuxuan Hu[3] and Fei Wang[4,*]

[1]Electric Power Research Institute of State Grid Hubei Corporation, Wuhan, China
[2]Hubei Key Laboratory of Regional New Power Systems and Rural Energy System Configuration, Wuhan, China
[3]Hubei Engineering Research Center of the Construction and Operation Control Technology of New Power Systems, Wuhan, China
[4]School of Electrical Engineering, Xi'an Jiao Tong University, Xi'an, China

*Corresponding Authors: Yiqun Kang. Email: kangyiqun343@126.com; Fei Wang. Email: wrjiao008@163.com

Received: 06 January 2026; Accepted: 28 February 2026; Published: 06 August 2026

ABSTRACT: As the world's energy framework shifts towards a low-carbon model, the widespread incorporation of renewable energy (RE) sources, primarily wind power and photovoltaics (PV), into the power grid is an unavoidable development. The micro-energy grid (MEG), as an integrated system that combines distributed energy, energy storage (ES), and power loads, can achieve efficient consumption of RE by implementing multi-machine optimal allocation and unified coordinated power control for parallel operation of grid-forming energy storage (GFES). For this purpose, this paper puts forward a low-carbon and economic dispatch strategy for MEG that considers multi-machine optimal allocation of GFES and unified coordinated power control for parallel operation. The strategy constructs a multi-machine optimal allocation model for GFES in the outer layer, striving to achieve the lowest operational costs for the MEG. In the inner layer, based on the obtained optimal multi-machine allocation scheme for GFES, a unified coordinated power control model for parallel operation of GFES in the MEG is constructed, targeting the minimization of pollutant gas emissions and system voltage deviation. The plant growth simulation algorithm (PGSA) is employed to solve the established models for multi-machine optimal allocation of GFES and unified coordinated power control for parallel operation in the MEG. Through simulation analysis, it has been substantiated that the proposed method can effectively achieve multi-machine optimal allocation and unified coordinated power control for parallel operation of GFES, reduce the operational costs of the MEG system, while also decreasing pollutant gas emissions and stabilizing system operation, thereby offering robust and substantial backing for the attainment of a low-carbon economy and the pursuit of sustainable development.

KEYWORDS: Grid-forming energy storage; unified coordinated power control; micro energy grid; plant growth simulation algorithm; low-carbon and economic dispatching strategy

1 Introduction

Against the backdrop of the world's proactive efforts to combat climate change and vigorously promote energy transition, the energy sector is undergoing unprecedented and profound transformations. The issues of environmental pollution and resource depletion caused by over-reliance on traditional fossil fuels are becoming increasingly severe, prompting countries around the world to turn their attention to clean and renewable RE sources [1]. Accelerating the establishment of a novel power system (PS) centered on RE has become an inevitable choice for the development of the times. Benefiting from their significant advantages, such as wide distribution, cleanliness, and pollution-free nature, RE sources like wind and PV power have seen a continuous rise in their proportion within the energy mix, and their large-scale integration into the PS has become an unstoppable trend [2,3].

However, the intermittent, volatile, and uncertain characteristics of RE pose enormous challenges to the stable operation of the PS. When the output of RE generation fluctuates significantly, it may lead to deviations in grid frequency and voltage, affecting the quality of power energy and even threatening the safety and stability of the grid. In this context, ES technology, as a key support for addressing RE consumption and ensuring the stable operation of the PS, has become increasingly prominent in its importance [4]. ES systems can store excess electrical energy when RE generation is abundant and release it when generation is insufficient, effectively smoothing out fluctuations in RE output and enhancing the reliability and flexibility of the PS. Among numerous ES technologies, GFES stands out with its unique technological advantages. Unlike traditional grid-following ES, GFES has the ability to autonomously establish voltage and frequency, and provide inertia support as well as voltage and frequency regulation services for the PS. It acts like a "stabilizer" for the PS, significantly enhancing the grid's anti-interference capability and recovery ability in scenarios with a high proportion of RE integration, thereby ensuring the stable and safe operation of the PS [5,6].

As an integrated system that combines distributed RE, ES systems, and power loads, the MEG is a crucial component of the new PS. Rational allocation of GFES and achieving unified coordinated control of its parallel operation power within the MEG are of paramount importance for improving the consumption capacity of RE, reducing the system operation cost, minimizing pollutant gas emissions, and promoting the development of a low-carbon economy [7]. Through multi-machine optimal allocation of GFES, the performance characteristics of different ES devices can be fully leveraged to achieve maximum resource utilization. Meanwhile, unified coordinated control of parallel operation power ensures collaborative work among various ES devices, enhancing the overall operational stability and efficiency of the system. Therefore, in-depth research on low-carbon economic dispatch strategies in MEGs that consider multi-machine optimal allocation of GFES and unified coordinated control of parallel operation power not only helps address the technical challenges brought about by large-scale integration of RE but also promotes the efficient operation and sustainable development of MEGs. It also provides important theoretical support and technological guarantees for the global transformation of energy and the achievement of low-carbon economic goals [8,9].

In the process of optimal configuration of GFES systems in microgrids, site selection needs to consider factors such as the geographical location of the microgrid, the distribution of RE generation, the distribution of loads, and the structure of the grid [10,11]. Determining the size of the GFES capacity requires consideration of the load characteristics of the microgrid, the characteristics of RE generation, and the cost and performance of the GFES system, with the goal of minimizing the investment and operational costs of the GFES system while meeting the microgrid's RE absorption needs [12–14]. Literature [15] establishes a multi-objective optimizing model for GFES optimization in microgrids based on minimizing user losses and environmental impact and simplifies the multi-objective optimizing problem into a single objective optimizing problem, which is solved using the maximum fuzzy satisfaction method. Literature [16] proposes a multi-objective optimizing model for GFES configuration in microgrids that considers RE utilization rate, network cost over the entire life cycle, and pollutant gas emission. It adopts a decimal elitist genetic algorithm for solution under the established strategies, achieving optimal dispatch of distributed RE and GFES systems. Literature [17] presents a GFES optimization dispatch and security-constrained unit model based on scenario optimization. Literature [18] utilizes Monte Carlo simulation and Latin hypercube techniques to simulate the uncertainty of wind power fluctuations and employs a computable algorithm to effectively solve the GFES optimization dispatch problem. Literature [19] proposes a joint optimization method for GFES capacity and power, aiming to minimize the investment cost of the GFES system and maximize RE absorption, which is addressed through the application of mixed-integer linear programming techniques. Literature [20] combines long-term capacity planning with short-term operational dispatch, proposing a multi-timescale coupled GFES system configuration model that uses stochastic programming to handle the uncertainty of wind and PV power output. Literature [21] presents a two-stage optimization strategy for GFES optimal configuration and operation. In the first stage, robust optimization is used to determine the GFES capacity, and in the follow-up step, model predictive control is employed to achieve real-time power allocation for the GFES system.

After determining the configuration of the GFES system, it is necessary to optimize the dispatch of its output in the MEG [22–24]. Literature [25] proposes an economic dispatch method for battery energy storage system (BESS) based on electricity market price signals, aiming to minimize system costs. It charges in periods of low electricity prices and discharges during periods of high prices, thereby reducing electricity costs. This dispatch method not only improves the economic efficiency of the BESS but also helps balance the supply and demand relationship of the grid. Literature [26] adjusts the discharging and charging strategies of the BESS according to changes in PS demand and proposes a BESS demand response dispatch method. During peak demand periods, it discharges to meet the peak demand, while during off-peak periods, it charges to store energy. This dispatch method helps reduce grid stress and improves the stability of the PS. Literature [27] achieves coordinated dispatch of GFES and multiple energy sources by enabling the GFES system within the microgrid to work synergistically with other RE resources. Through coordinated dispatch, the advantages of various energy resources can be entirely utilized, enhancing the overall effectiveness and dependability of the complete energy network. Literature [28] utilizes advanced forecasting techniques to predict the supply and demand situation of the PS and optimizes the dispatch of the GFES system based on the forecasting results. This method can reduce energy waste and enhance the operational productivity of the PS. With precise forecasting, the GFES system can charge and discharge at the most appropriate times, thereby maximizing its effectiveness. Literature [29] proposes an optimization dispatch strategy for distributed PV-storage systems based on the output characteristics of PV power. This strategy primarily targets distributed GFES systems that include PV power sources. By continuously updating short-term load demand information on the grid side and forecasting the output of distributed PV power generation, it enhances the precision of dispatching GFES modules on the user side. Simultaneously, considering time-of-use electricity prices, combined with the state of charge of the GFES system and PV output information, it determines the optimal dispatch strategy for the PV-storage system to improve the overall revenue of the system [30–32].

However, existing research still exhibits notable limitations. On one hand, most studies optimize the long-term capacity configuration and short-term coordinated operation of energy storage as two separate processes, overlooking the bidirectional coupling relationship between them and making it difficult to achieve comprehensive optimization throughout the entire lifecycle. On the other hand, at the operational control level, research predominantly focuses on single objectives such as economic efficiency or reliability. Although environmental benefits are occasionally considered, they are often converted into economic costs. Meanwhile, in the context of multi-machine parallel scenarios for GFES, there is a lack of unified coordinated control strategies capable of synergistically optimizing the dual objectives of low carbon emissions and voltage stability. Therefore, establishing a two-layer collaborative framework that integrates "planning-operation" to optimize the multi-machine configuration of GFES while achieving multi-objective coordinated control for low-carbon and economically stable operation remains an urgent issue to be addressed.

To fill the current research gap and promote the effective consumption of RE, this paper puts forward a low-carbon and economic dispatch strategy considering optimal multi-machine allocation and unified coordinated power control for parallel operation of GFES in MEG. The main contributions of this paper are as follows:

1. A double-layer low-carbon and economic dispatching model for MEG is proposed, which integrates the optimization configuration and operation of GFES.
2. At the outer layer, an optimization model for GFES configuration in MEG is constructed with the objective of minimizing the operational costs for the MEG. At the inner layer, based on the obtained GFES configuration scheme, an optimization dispatch model for GFES in MEG is developed, aiming to minimize both pollutant gas emissions and system voltage deviations.
3. To solve the proposed double-layer dispatching model for GFES configuration and operation in MEG, the PGSA is employed for both layers. Simulations are conducted based on a specific MEG to ascertain and confirm the efficacy of the proposed approach.

2 Optimal Configuration and Operation Model of GFES in MEG

2.1 The Optimal Configuration Model of GFES

In the process of optimal configuration for GFES, the installation position, rated power and capacity of GFES in the system are mainly needed to be determined. The rated power and capacity constraints of GFES configuration are:

$$P_{es,\min} \le P_{es,i} \le P_{es,\max} \tag{1}$$

$$E_{es,\min} \le E_{es,i} \le E_{es,\max} \tag{2}$$

where: $P_{es,i}$ is rated power of GFES installed at bus i; $P_{es,\min}$ and $P_{es,\max}$ denote the lower and upper limits of rated power for GFES, respectively; $E_{es,i}$ is rated GFES capacity installed at bus i; $E_{es,\min}$ and $E_{es,\max}$ denote the lower and upper limits of GFES capacity, respectively.

The installation quantity of GFES is limited as follows:

$$n_{ins} \le n_{\max} \tag{3}$$

where: n_{ins} is the actual installed number of GFES; $n_{\max}$ is the largest installed number of GFES.

2.2 The Optimal Operation Model of GFES

In the process of optimal operation for GFES, the output power of GFES is mainly needed to be determined. According to the operation characteristics of GFES, the stored energy $E(t+1)$ at time $t+1$ depends on the stored energy $E(t)$ and the charging or discharging power $P(t)$ at time t. When GFES is in the process of charging ($P(t) < 0$):

$$E\left(t+1\right) = E\left(t\right) - \eta_c P\left(t\right) \Delta t \tag{4}$$

where: $E(t+1)$ denotes the stored energy at time $t+1$; $E(t)$ is the stored energy at time t; $P(t)$ is the charging or discharging power ($P(t) < 0$ means charging, $P(t) > 0$ means discharging); η_c is the charging efficiency; $\triangle t$ is the time interval.

When GFES is in the process of discharging ($P(t) > 0$):

$$E\left(t+1\right) = E\left(t\right) - \frac{P\left(t\right) \Delta t}{\eta_d} \tag{5}$$

where: η_d is the discharging efficiency.

The charging/discharging power of GFES should be smaller than the maximum charging/discharging power:

$$P_{c,i}\left(t\right) \le P_{c,\max} \tag{6}$$

$$P_{d,i}\left(t\right) \le P_{d,\max} \tag{7}$$

where: $P_{d,i}(t)$ and $P_{c,i}(t)$ denote the discharging and charging power at time t; $P_{d,\max}$ and $P_{c,\max}$ denote the maximum discharging and charging power.

The state of charge (SOC) of GFES is:

$$S_{oc,i}\left(t\right) = \frac{E\left(t\right)}{E_{es,i}} \tag{8}$$

where: $S_{oc,i}\left(t\right)$ denotes the SOC of GFES at time t.

The SOC of GFES is the same at the initial time and the end time of scheduling:

$$S_{oc,i}\left(0\right) = S_{oc,i}\left(24\right) \tag{9}$$

where: $S_{oc,i}\left(0\right)$ and $S_{oc,i}\left(24\right)$ denote the SOC of GFES at the initial time and the end time.

The constraint of SOC for GFES is:

$$S_{oc,\min} \le S_{oc,i}\left(t\right) \le S_{oc,\max} \tag{10}$$

where: $S_{oc,\min}$ and $S_{oc,\max}$ are the minimum and maximum values of the SOC, respectively.

In this paper, to prevente a substantial quantity of non-viable solutions caused by overcharge or overdischarge of GFES system, the overcharge or overdischarge of GFES system is treated as follows: when the battery is overcharged ($P(t) < 0$), calculate the stored energy according to Formula (4), and if $E(t + 1) > E_{\max}$, adjust $P(t)$ at this time:

$$P\left(t\right) = \frac{E\left(t\right) - E_{\max}}{\eta_c \Delta t} \tag{11}$$

where: $E_{\max}$ is the maximum value of remaining energy for GFES.

When the battery is over-discharged ($P(t) > 0$), calculate the stored energy according to Formula (5), and if $E(t + 1) < E_{\min}$, adjust $P(t)$ at this time:

$$P\left(t\right) = \frac{\left(E\left(t\right) - E_{\min}\right)\eta_d}{\Delta t} \tag{12}$$

where: $E_{\min}$ is the minimum value of remaining energy for GFES.

3 Double-Layer Model for Optimal Configuration and Operation of GFES in MEG

3.1 Outer Layer Model for Optimal GFES Configuration

In the outer layer optimal configuration model for GFES, the state variable to be determined are the installation position, rated power and capacity of GFES in the system, and the objective function (OF) is the minimum daily operation cost of MEG, which is shown as follows:

$$\min \quad F_c = F_{c,grid} + F_{c,fuel} + F_{c,green} + F_{c,penalty} + F_{c,es,inv} + F_{c,es,pro} \tag{13}$$

where: F_c is the daily operation cost of MEG; $F_{c,grid}$ is the cost of purchasing electricity from power grid in MEG; $F_{c,green}$ is the power generation cost of RE sources; $F_{c,fuel}$ is the fuel cost of gas turbine in MEG; $F_{c,penalty}$ is the RE rejection penalty cost; $F_{c,es,inv}$ is the average daily operation cost of GFES investment; $F_{c,es,pro}$ is the profit of peak-valley price difference in daily operation of GFES.

The specific calculation expressions of various expenses are as follows:

$$\begin{cases} F_{c,grid} = \lambda_{grid} \sum_{t=1}^{24} P_{grid}(t) \\ F_{c,fuel} = \lambda_{fuel} \sum_{t=1}^{24} \dfrac{P_{fuel}(t)}{\eta_{fuel}\gamma_{fuel}} \\ F_{c,green} = \lambda_{green} \sum_{t=1}^{24} P_{green}(t) \\ F_{c,penalty} = \lambda_{penalty} \sum_{t=1}^{24} P_{penalty}(t) \\ F_{c,es,inv} = \dfrac{\dfrac{r(1+r)^y}{(1+r)^y - 1} \sum_{i=1}^{N} \left(\lambda_{es,e} E_{i,rated} + \left(\lambda_{es,p} + \lambda_{es,m} \right) P_{i,rated} \right)}{365} \\ F_{c,es,pro} = \lambda_{es,differ} E_{es,work} \end{cases} \tag{14}$$

where: λ_{grid} is electricity price of MEG purchasing electricity from PS; $P_{grid}(t)$ denotes the power which is purchased from the MEG; λ_{fuel} is natural gas price; $P_{fuel}(t)$ denotes the electric power generated by gas turbine in MEG; η_{fuel} is gas turbine power generation efficiency; γ_{fuel} denotes the calorific value for natural gas; λ_{green} is the unit power generation cost of RE sources; $P_{green}(t)$ denotes the power generated by RE; $\lambda_{penalty}$ is the unit penalty cost of RE abandoning electricity; $P_{penalty}(t)$ is the abandoning power of RE sources; r denotes the annual interest rate of funds; y is the service life of GFES; N denotes the total number of GFES installations; $E_{i,rated}$ is the rated capacity of the i-th GFES; $P_{i,rated}$ is the rated power of the i-th GFES; $\lambda_{es,e}$ is the unit capacity cost of GFES; $\lambda_{es,p}$ denotes the unit power cost of GFES; $\lambda_{es,m}$ is the unit power maintenance and operation cost of GFES; $\lambda_{es,differ}$ peak-valley price difference of GFES operation; $E_{es,work}$ is the daily charge or discharge capacity during GFES operation.

3.2 Inner Layer Model for Optimal GFES Operation

In the inner layer model for optimal GFES operation, the state variable to be determined is the output power of GFES and the output power of other resources. The OF of inner layer model are the lowest emission of polluting gas and bus voltage violation, which are shown as follows:

$$\begin{aligned} \min \quad F_e = & \sum_{t=1}^{24} \left[\left(\mu_{CO_2,f} + \mu_{NO_x,f} + \mu_{SO_x,f} \right) \frac{P_{fuel}(t)}{\eta_{fuel}\gamma_{fuel}} \right] \\ & + \sum_{t=1}^{24} \left[\left(\mu_{CO_2,e} + \mu_{NO_x,e} + \mu_{SO_x,e} \right) \gamma_e P_{grid}(t) \right] \end{aligned} \tag{15}$$

$$\min \quad F_v = \sum_{t=1}^{24} \sum_{k=1,k\neq s}^{n_{bus}} \left| \frac{\Delta U_k(t)}{U_{k,\max} - U_{k,\min}} \right| \tag{16}$$

where: F_e is the emission of polluted gas; F_v is the bus voltage violation; $\mu_{CO_2,f}$, $\mu_{NO_x,f}$ and $\mu_{SO_x,f}$ are the emission coefficients of CO_2, NO_x, and SO_x generated by gas turbine; $\mu_{CO_2,e}$, $\mu_{NO_x,e}$ and $\mu_{SO_x,e}$ are the emission coefficients of CO_2, NO_x, and SO_x which are generated by electric energy; γ_e denotes the transformer efficiency of electric energy; n_{bus} is the total bus number of the MEG; $U_{k,\max}$ and $U_{k,\min}$ denote the maximum and the minimum allowable voltage of bus k; $\Delta U_k(t)$ denotes the voltage violation of bus k at time t; s represents the slack bus.

For $\Delta U_k(t)$, the calculation formula is as follows:

$$\begin{cases} \Delta U_k(t) = U_{k,\min} - U_k(t), & U_k(t) \le U_{k,\min} \\ \Delta U_k(t) = 0, U_{k,\min} \le U_k(t) \le U_{k,\max} & \\ \Delta U_k(t) = U_k(t) - U_{k,\max}, & U_k(t) \ge U_{k,\max} \end{cases} \tag{17}$$

In order to simplify the OF of the inner layer model, the OF of voltage deviation is taken as the penalty term, so that the inner layer model of multi OF is transformed to a single OF model. The formula is as follows:

$$\begin{cases} \min \quad F_{inner} = \overline{F}_e + \overline{\lambda}_v \overline{F}_v \\ \overline{F}_e = \frac{F_e - F_{e,\min}}{F_{e,\max} - F_{e,\min}} \\ \overline{F}_v = \frac{F_v - F_{v,min}}{F_{v,\max} - F_{v,\min}} \end{cases} \tag{18}$$

where: F_{inner} is the extended OF for inner layer model in MEG; $\overline{\lambda}_v$ is the penalty factor (it is taken as 1 in this paper); $\overline{F}_e$ is the normalized emission of polluted gas; $\overline{F}_v$ is the normalized bus voltage violation; $F_{e,\max}$, $F_{e,\min}$, and $F_{v,\max}$, $F_{v,\min}$ are the estimated maximum and minimum values of polluted gas emission and voltage deviation obtained through preliminary simulation or theoretical analysis, respectively.

3.3 The Constraints of MEG System

The relevant constraints of the GFES system have been given in the part II, and the constraints of other parts in MEG are given here. Power balance constraint of MEG is as follows:

$$P_{grid}(t) + P_{fuel}(t) + P_{green}(t) = P(t) + P_{load}(t) \tag{19}$$

where: $P_{load}(t)$ is the load power at time t.

RE consumption constraint is as follows:

$$\sum_{t=1}^{24} P_{green}(t) = \eta_{pre} \sum_{t=1}^{24} P_{green,pre}(t) \tag{20}$$

where: η_{pre} is the RE consumption rate; $P_{green,pre}(t)$ is the predictive power value of RE.

Power generation constraint of gas turbine is as follows:

$$P_{fuel}^{down} \le P_{fuel}(t) \le P_{fuel}^{up} \tag{21}$$

where: P_{fuel}^{down} and P_{fuel}^{up} denote the lower and upper limit of gas turbine power, respectively.

4 Optimal Dispatching Method of MEG Based on PGSA

As an intelligent algorithm, PGSA has shown outstanding global search ability, calculation accuracy and stability in solving various engineering optimization problems since it was put forward. Inspired by the phototropism mechanism of plants, the PGSA regards the solution space of an optimization problem as the growth habitat for plants, and the optimal solution as the light source that guides plant growth. It simulates the real phototropism mechanism of plants and establishes a growth pattern where branches and leaves grow rapidly under different light intensity conditions. Through continuous iterations, it simulates the rapid spreading of plant branches within the solution space until the optimal solution is found.

Assuming the plant grows a stem out of the root node (denoted as B_0), and the stem has k nodes which exhibit superior environmental adaptability in comparison to the root node. Let the environmental adaptability function of each node is g (In this paper, g refers to the objective function, i.e., Eqs. (13) and (18)), then the fitness C_{Mi} at node B_{Mi} is:

$$C_{Mi} = \frac{g\left(B_0\right) - g\left(B_{Mi}\right)}{\sum\limits_{j=1}^{k}\left(g\left(B_0\right) - g\left(B_{Mj}\right)\right)}, \quad i = 1, 2, \ldots, k \tag{22}$$

where: C_{Mi} is the fitness at node B_{Mi}; $g(B_0)$ is the adaptability of root node B_0; $g(B_{Mi})$ is the adaptability of node B_{Mi}.

It can be concluded from Eq. (22) that the suitability values of all nodes are confined to the interval $[0, 1]$. According to the principle of random numbers, the priority node for the next growth branch can be selected within this interval. On the newly generated branch, a quantity of q new nodes are produced. Subsequently, the fitness values of all nodes present on the plant can undergo a recalculation process:

$$C_{Mi} = \frac{g\left(B_0\right) - g\left(B_{Mi}\right)}{\Delta_1 + \Delta_2}, \qquad i = 1, 2, \ldots, k \tag{23}$$

$$C_{Mj} = \frac{g\left(B_0\right) - g\left(B_{Mj}\right)}{\Delta_1 + \Delta_2}, \qquad j = 1, 2, \ldots, q \tag{24}$$

$$\Delta_1 = \sum_{l=1}^{k}\left(g\left(B_0\right) - g\left(B_{Ml}\right)\right) \tag{25}$$

$$\Delta_2 = \sum_{l=1}^{q}\left(g\left(B_0\right) - g\left(B_{Ml}\right)\right) \tag{26}$$

where: C_{Mj} is the fitness at node B_{Mj}; $g(B_{Mj})$ is the adaptability of node B_{Mj}; $g(B_{Ml})$ is the adaptability of node B_{Ml}.

The above branching process is iterated repeatedly until the preset number of terminating iterations is reached. The implementation steps of PGSA are as follows:

1. Set the values of the maximum iteration number $T_{\max}$ and the branch length;
2. Set the initial iteration number $T = 1$, generate initial root node at B_0 position, and define k node positions on the stem from the root node B_0;
3. Calculate the fitness of each node on Eq. (22), and the position of the node with the highest fitness is stored;
4. Select a branch node and add 2n lateral branches to this node, update the fit-ness of each node on the plant based on Eqs. (23) and (24), and replace the best position if the new node has higher fitness than all other nodes;
5. Iteratively execute steps (3) and (4) until the predefined maximum number of iterations has been reached.

The flow chart of optimal dispatching method in MEG based on PGSA is shown in Fig. 1. The double-layer optimization model is shown in Fig. 2.

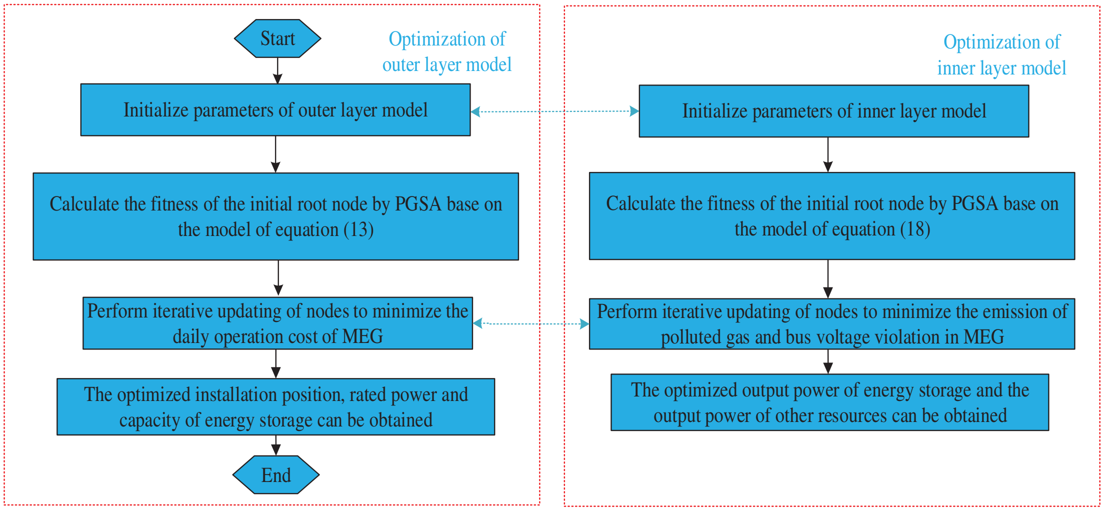

Figure 1: The flow chart of optimal dispatching method in MEG based on PGSA.

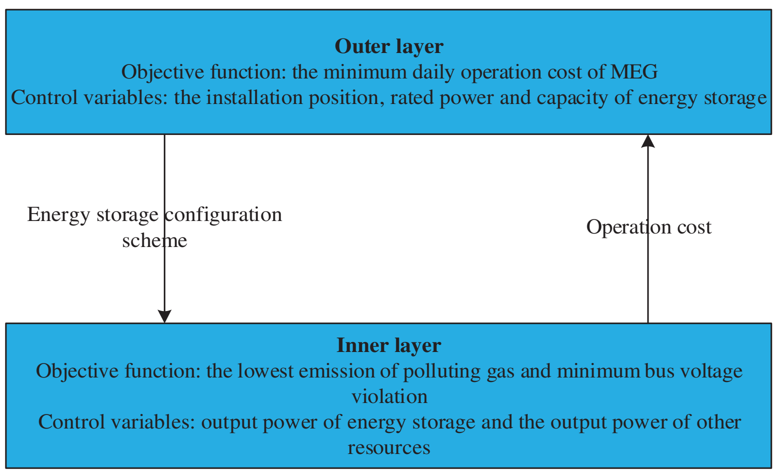

Figure 2: The double-layer optimization model.

5 Numerical Test and Analysis

5.1 Basic Data and Simulation Conditions

To substantiate the efficacy of the methodology introduced in this study, a micro energy grid system is constructed based on the IEEE-13-bus system. IEEE-13 bus distribution system circuit diagram is shown in Fig. 3. The original system is an unbalanced grounded system with a neutral conductor, where bus 1 serves as the balanced bus, buses 5, 7, and 8 are contact buses, and the remaining buses are load buses. This paper focuses on the optimal allocation and optimal operation of GFES in the micro energy grid. The following simplifications are made to the original system: the neutral conductor, transformer branches, and shunt capacitance branches of lines are not considered, and it is assumed that all branches have the same type and phase spacing (with branch parameters adopting those of branch 1–2 in the original system). Distributed PV are connected to buses 8, 11, and 13, a 0.2 MW miniature gas turbine is connected to bus 5, and bus 1 serves as the grid connection bus. Based on the proposed double-layer dispatching model in this paper, research on the optimal allocation and operation of GFES is conducted in this micro energy grid system. The allowable number of distributed GFES installations is 2, and the GFES is charged and discharged once every working day, and the charging and discharging efficiency is 0.95.

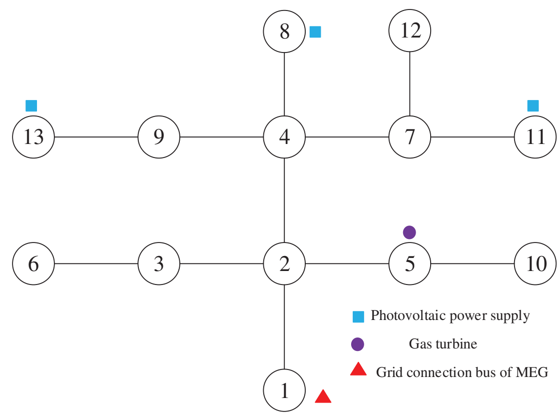

Figure 3: The IEEE-13 bus distribution system circuit diagram.

5.2 Simulation Results and Analysis

In order to highlight the superiority of the method proposed in this paper, a comparison is made between the proposed method and genetic algorithm (GA), bat algorithm (BA), and particle swarm optimization (PSO) algorithm. As the research in this paper is a multi-objective optimization problem, the obtained solution is a Pareto solution set (PSS), and the PSS obtained by the proposed method, GA, PSO and BA are shown in Fig. 4.

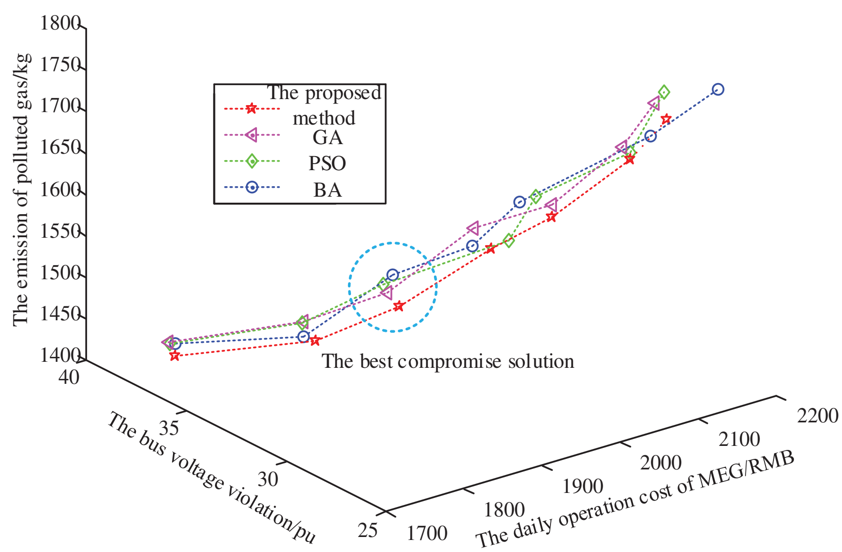

Figure 4: The PSS of various method.

Seen from Fig. 4, the PSS obtained by the proposed method is obviously superior to the other three methods in general. In addition, in order to compare the differences of optimization results by different methods, the comparison of the best compromise solutions obtained by various methods are shown in Table 1. Under the best compromise solution, the configuration of GFES in different algorithms are shown in Fig. 5.

Table 1: The comparative analysis of the optimal compromise solutions.

Method	Daily Operation Cost/RMB	Emission of Polluted Gas/kg	Bus Voltage Violation/p.u.	The Total Number of Iterations	The Average Single Iteration Time (s)	The Total Iteration Time (s)
GA	1892	1519	32.46	112	1.5	168.0
PSO	1897	1523	32.88	135	1.2	162.0
BA	1917	1525	33.19	102	1.6	163.2
The proposed method	1889	1512	31.77	85	1.8	153.0

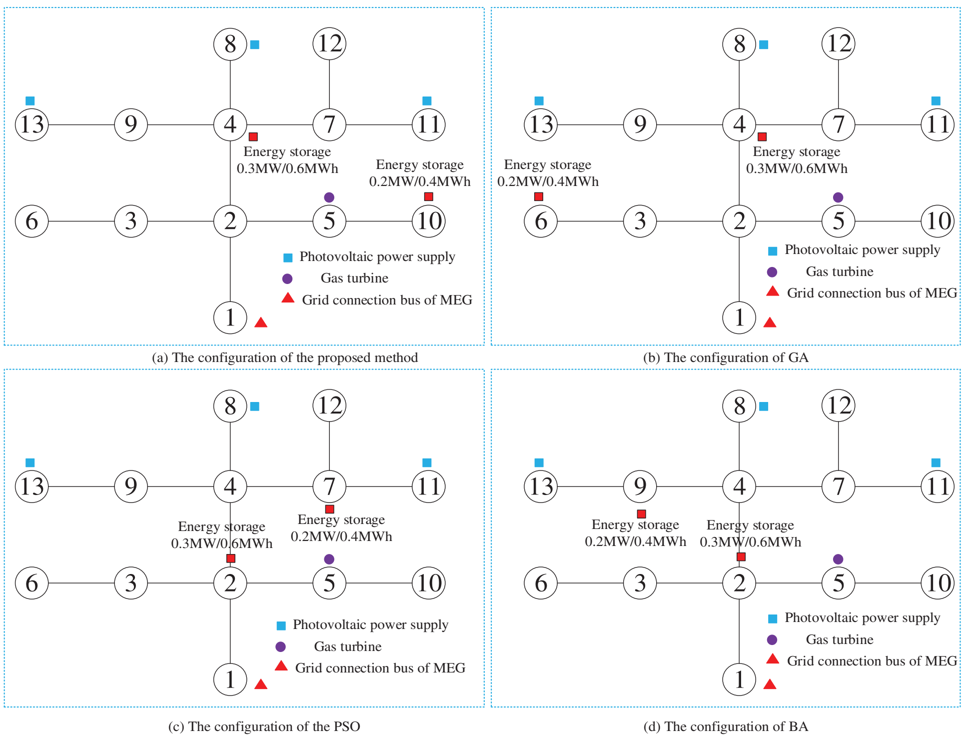

Figure 5: The configuration of GFES in the best compromise solutions.

Seen from Table 1, daily operation cost, emission of polluted gas and bus voltage violation of the optimal compromise solution under GA algorithm are 1892 RMB, 1519 kg and 32.46 p.u., respectively; daily operation cost, emission of polluted gas and bus voltage violation of the optimal compromise solution under PSO algorithm are 1897 RMB, 1523 kg and 32.88 p.u., respectively; daily operation cost, emission of polluted gas and bus voltage violation of the optimal compromise solution under BA algorithm are 1917 RMB, 1525 kg and 33.19 p.u., respectively; daily operation cost, emission of polluted gas and bus voltage violation of the optimal compromise solution under the proposed method are 1889 RMB, 1512 kg and 31.77 p.u., respectively. Therefore, the method proposed in this paper has the smallest indexes and the best effect. In addition, when considering the number of convergence iterations and convergence time, the overall performance of the method proposed in this paper is also the best.

Based on Fig. 5, it is evident that the total GFES capacity configured by each algorithm is the same, all being 0.5 MW/1.0 MWh, but the locations of the GFES configurations differ. The method proposed in this paper involves connecting 0.3 MW/0.6 MWh to bus 4 and 0.2 MW/0.4 MWh to bus 10; for GA, it is 0.3 MW/0.6 MWh to bus 4 and 0.2 MW/0.4 MWh to bus 6; for PSO, it is 0.3 MW/0.6 MWh to bus 2 and 0.2 MW/0.4 MWh to bus 7; and for BA, it is 0.3 MW/0.6 MWh to bus 2 and 0.2 MW/0.4 MWh to bus 9.

Table 2 further gives the comparison of the results with single objective optimization of traditional model under different algorithms.

Table 2: A comprehensive comparative analysis of the optimization outcomes yielded by distinct algorithms.

Method		The Proposed Method	GA	PSO	BA
Economical and environmental optimal solution (double-level collaborative optimization)	Daily operation cost/RMB	1743	1757	1748	1749
	Emission of polluted gas/kg	1426	1429	1435	1437
	Bus voltage violation/pu	37.25	38.11	37.72	37.51
Operational optimal solution (single objective optimization of traditional model)	Daily operation cost/RMB	2113	2117	2123	2190
	Emission of polluted gas/kg	1731	1741	1757	1742
	Bus voltage violation/pu	27.14	27.89	27.62	27.52

As can be seen from Table 2, when both are based on the PGSA algorithm, for the traditional model that primarily considers optimal operation, the daily operating cost under single-objective optimization is 2113 RMB, and the pollutant gas emissions are 1731 kg. In contrast, for the double-layer model proposed in this paper, which primarily considers both economic and environmental optimality, the daily operating cost under multi-objective optimization is 1743 RMB, and the pollutant gas emissions are 1426 kg. The daily operating cost decreases by 17.51%, and the pollutant gas emissions decrease by 17.62%, achieving an overall better outcome. In addition, it is evident from Table 2 that the index of the method proposed in this paper is still the smallest in various algorithms, which subsequently serves as further corroboration of the validity of the approach put forth in this study.

6 Conclusions

To address the challenges of the global low-carbon transition in energy structure and promote the efficient accommodation of RE in micro-energy networks, this paper proposes a low-carbon economic dispatch strategy for micro-energy networks that considers the multi-machine optimal configuration and unified coordinated power control of GFES. The main contributions of this study are as follows:

1. A novel "configuration-control" double-layer optimization framework integrating planning and operation is proposed. This framework breaks away from the traditional paradigm of studying the long-term configuration and short-term scheduling of energy storage separately. Through closed-loop coupling of the inner and outer models, it achieves systematic optimization of the comprehensive benefits throughout the entire lifecycle.
2. A GFES optimization scheduling model oriented towards multi-objective synergy is constructed. In the outer level, the multi-machine configuration of GFES is optimized with the objective of minimizing the total system operating cost. In the inner level, a unified coordinated power control model for multi-GFES is innovatively established with the dual objectives of minimizing pollutant emissions and system voltage deviation, clearly defining the collaborative optimization path for low-carbon and stable operation.

By uniformly applying PGSA to solve the inner and outer models and comparing it with multiple classical optimization algorithms, simulation analysis indicates that the proposed strategy can effectively reduce the operational cost of the micro-energy grid system by 17.51%, simultaneously decrease pollutant gas emissions by 17.62%, and stabilize the system voltage, providing robust decision-making support for the power system to achieve a low-carbon economy and sustainable development.

Acknowledgement: Thanks for the support from the Science and technology projects of State Grid Hubei Corporation.

Funding Statement: This work was supported by the Science and Technology Projects of State Grid Hubei Corporation, Project No. 52153224002D.

Author Contributions: Conceptualization, Yiqun Kang, Zhe Li, Li You, Haozhe Xiong, Yuxuan Hu, Fei Wang; methodology, Yiqun Kang, Zhe Li, Li You, Haozhe Xiong, Yuxuan Hu, Fei Wang; software, Yiqun Kang, Zhe Li, Li You, Haozhe Xiong, Yuxuan Hu, Fei Wang; validation, Yiqun Kang, Zhe Li, Li You, Haozhe Xiong, Yuxuan Hu, Fei Wang; formal analysis, Yiqun Kang, Zhe Li, Li You, Haozhe Xiong, Yuxuan Hu, Fei Wang; investigation, Yiqun Kang, Zhe Li, Li You, Haozhe Xiong, Yuxuan Hu, Fei Wang; writing—original draft preparation, Yiqun Kang, Zhe Li, Li You, Haozhe Xiong, Yuxuan Hu, Fei Wang. All authors reviewed and approved the final version of the manuscript.

Availability of Data and Materials: The authors confirm that the data supporting the findings of this study are available within the article.

Ethics Approval: This study did not involve human participants, animal subjects, or any clinical data. Therefore, ethical review and approval were not required for this research.

Conflicts of Interest: The authors declare no conflicts of interest.

References

1. Wu X, Liu L, Wu Y, Luo C, Tang Z, Kerekes T. Near-optimal energy management strategy for a grid-forming PV and hybrid energy storage system. IEEE Trans Smart Grid. 2025;16(2):1422–33. doi:10.1109/tsg.2024.3509642.
2. Zhang K, Shi M, Chen X, Shao D, Xu Y, Chen Y. Interaction modeling and stability analysis of grid-forming energy storage system based on SISO transfer functions. IEEE Trans Sustain Energy. 2025;16(1):573–87. doi:10.1109/TSTE.2024.3471801.
3. Wang F, Xu J, Li G. A variable virtual impedance current limitation strategy of grid-forming energy storage-STATCOM. IEEE Trans Power Deliv. 2024;39(6):3450–61. doi:10.1109/TPWRD.2024.3476913.
4. Perez-Basante A, de Muro AG, Ordono A, Ceballos S, Unamuno E, Barrena JA. A tuning method for the supplementary voltage controller of dual-side grid forming converters in distributed storage systems. IEEE Open J Ind Electron Soc. 2025;6:202–15. doi:10.1109/OJIES.2025.3533022.
5. Zhang H, Xiang W, Wen J. Dual grid-forming control with energy regulation capability of MMC-HVDC system integrating offshore wind farms and weak grids. IEEE Trans Power Syst. 2024;39(1):261–72. doi:10.1109/TPWRS.2023.3244807.
6. Zhang H, Zhou S, Gu W, Zhu C, Chen XG. Optimal operation of micro-energy grids considering shared energy storage systems and balanced profit allocations. CSEE J Power Energy Syst. 2023;9(1):254–71.
7. Liao YH, Lai WR, Yu MH, Lin TH. Power regulation strategy of grid-forming bidirectional interlinking converters in hybrid AC-DC microgrid with energy storage management. IEEE Access. 2025;13:35401–16. doi:10.1109/ACCESS.2025.3543888.
8. Zheng L, Wang J, Chen J, Ye C, Gong Y. Two-stage co-optimization of a park-level integrated energy system considering grid interaction. IEEE Access. 2023;11:66400–14. doi:10.1109/ACCESS.2023.3290160.
9. Wu D, Lu Z, Tan J, Lin T, Liu Y, Wang K. A feedback analytic algorithm for maximal solar energy harvesting of InP stepped nanocylinders. IEEE Photonics J. 2024;16(1):2700109. doi:10.1109/JPHOT.2024.3353787.

10. Luo Y, Yuan H, Hu Z, Yang D, Zhang H. Optimal scheduling of micro-energy grid based on Pareto frontier under uncertainty and pollutant emissions. IEEE Trans Smart Grid. 2024;15(1):368–80. doi:10.1109/TSG.2023.3273816.
11. Yang Y, Yang P, Zhao Z, Lai LL. A multi-timescale coordinated optimization framework for economic dispatch of micro-energy grid considering prediction error. IEEE Trans Power Syst. 2024;39(2):3211–26. doi:10.1109/TPWRS.2023.3274751.
12. Li Z, Li P, Xia J, Liu X. Optimization for micro-energy grid dispatch based on non-supplementary fired compressed air energy storage aided energy hub and hybrid hyper-spherical search. J Mod Power Syst Clean Energy. 2022;10(4):1009–20. doi:10.35833/MPCE.2020.000639.
13. Dey B, Jadav R, Kumar RS. Choice of an efficient, sustainable and cost-effective energy storage system for optimal operation of a microgrid system incorporating adaptive demand side management strategies. J Energy Storage. 2025;139(2):118896. doi:10.1016/j.est.2025.118896.
14. Luo Y, Hao H, Yang D, Yin Z, Zhou B. Optimal operation strategy of combined heat and power system considering demand response and household thermal inertia. IEEE Trans Consum Electron. 2023;69(3):366–76. doi:10.1109/TCE.2023.3250276.
15. Nozarian M, Fereidunian A, Barati M. Reliability-oriented planning framework for smart cities: from interconnected micro energy hubs to macro energy hub scale. IEEE Syst J. 2023;17(3):3798–809. doi:10.1109/JSYST.2023.3244498.
16. Ha T, Xue Y, Lin K, Zhang Y, Van Thang V, Nguyen T. Optimal operation of energy hub based micro-energy network with integration of renewables and energy storages. J Mod Power Syst Clean Energy. 2022;10(1):100–8. doi:10.35833/mpce.2020.000186.
17. Feng S, Wei W, Chen Y. Day-ahead scheduling and online dispatch of energy hubs: a flexibility envelope approach. IEEE Trans Smart Grid. 2024;15(3):2723–37. doi:10.1109/TSG.2023.3337629.
18. Kuraganti M, Chinthamalla R. A novel transformer less ultra gain DC-DC converter for renewable micro energy sources. IEEE Lat Am Trans. 2024;22(8):695–703. doi:10.1109/TLA.2024.10620415.
19. Seifossadat SA, Rastegar M, Mohammadi M, Senemmar S, Zhang J. Hierarchical microenergy hub sizing and placement in integrated electricity and natural gas distribution systems. IEEE Syst J. 2022;16(4):5380–91. doi:10.1109/JSYST.2021.3136586.
20. Li J, Fang Z, Wang Q, Zhang M, Li Y, Zhang W. Optimal operation with dynamic partitioning strategy for centralized shared energy storage station with integration of large-scale renewable energy. J Mod Power Syst Clean Energy. 2024;12(2):359–70. doi:10.35833/mpce.2023.000345.
21. Shi Z, Wang W, Huang Y, Li P, Dong L. Simultaneous optimization of renewable energy and energy storage capacity with the hierarchical control. CSEE J Power Energy Syst. 2022;8(1):95–104. doi:10.17775/cseejpes.2019.01470.
22. Li X, Wang S. Energy management and operational control methods for grid battery energy storage systems. CSEE J Power Energy Syst. 2021;7(5):1026–40. doi:10.17775/cseejpes.2019.00160.
23. Abomazid AM, El-Taweel NA, Farag HEZ. Optimal energy management of hydrogen energy facility using integrated battery energy storage and solar photovoltaic systems. IEEE Trans Sustain Energy. 2022;13(3):1457–68. doi:10.1109/TSTE.2022.3161891.
24. Liu Y, Han X, Xing Z, Li P, Liu H, Jiang Z. Research on control strategy of hybrid superconducting energy storage based on reinforcement learning algorithm. IEEE Trans Appl Supercond. 2024;34(8):1–4. doi:10.1109/tasc.2024.3420314.
25. Tendulkar SG. Optimized electricity price prediction for battery energy storage system (BESS) scheduling. In: 2025 International Conference on Advanced Computing Technologies (ICoACT); 2025 Mar 14–15; Sivalasi, India. p. 1–7. doi:10.1109/ICoACT63339.2025.11004771.
26. Manojkumar R, Inala KP. Rule-based peak shaving using battery energy storage with a case study analysis. In: 2024 2nd International Conference on Cyber Physical Systems, Power Electronics and Electric Vehicles (ICPEEV); 2024 Sep 26–28; Hyderabad, India. p. 1–6. doi:10.1109/ICPEEV63032.2024.10932080.
27. Tanis Z, Durusu A. Cooperative behaviors and multienergy coupling through distributed energy storage in the peer-to-peer market mechanism. IEEE Access. 2025;13:12081–102. doi:10.1109/ACCESS.2025.3529205.

28. Mugyema M, Kamper MJ, Wang RJ, Sebitosi BA. Performance and cost comparison of drive technologies for a linear electric machine gravity energy storage system. IEEE Access. 2024;12:46953–66. doi:10.1109/ACCESS.2024.3383161.
29. Chegari B, Tabaa M, Simeu E, El Ganaoui M. Optimal energy management of a hybrid system composed of PV, wind turbine, pumped hydropower storage, and battery storage to achieve a complete energy self-sufficiency in residential buildings. IEEE Access. 2024;12:126624–39. doi:10.1109/ACCESS.2024.3454149.
30. Hossain MB, Islam MR, Muttaqi KM, Sutanto D, Agalgaonkar AP. Component sizing and energy management for a supercapacitor and hydrogen storage based hybrid energy storage system to improve power dispatch scheduling of a wind energy system. IEEE Trans Ind Appl. 2025;61(1):872–83. doi:10.1109/TIA.2024.3477417.
31. Dey B, Khumanleima Chanu L, Sharma G, Bokoro PN, Bansal RC, Kumar R. Economic operation of a microgrid system with amalgamated load shifting/curtailing policy and smart PHEV charging. Energy. 2025;334(2):137824. doi:10.1016/j.energy.2025.137824.
32. Cheng X, Wu T, Yao W, Yang Y. Selection method for new energy output guaranteed rates considering optimal energy storage configuration. CSEE J Power Energy Syst. 2024;10(2):539–47. doi:10.17775/cseejpes.2020.03330.